

**UCLA**

**Adaptive Optics for Extremely Large Telescopes 4 - Conference Proceedings**

**Title**

Resolving the low-mass content of Westerlund 1 using MCAO

**Permalink**

<https://escholarship.org/uc/item/1df66431>

**Journal**

Adaptive Optics for Extremely Large Telescopes 4 - Conference Proceedings, 1(1)

**Authors**

Andersen, Morten  
Neichel, Benoit  
Bernard, Anais

**Publication Date**

2015

**DOI**

10.20353/K3T4CP1131603

**Copyright Information**

Copyright 2015 by the author(s). All rights reserved unless otherwise indicated. Contact the author(s) for any necessary permissions. Learn more at <https://escholarship.org/terms>

Peer reviewed

# Resolving the low-mass content of Westerlund 1 using MCAO

M. Andersen<sup>a</sup>, B. Neichel<sup>b</sup>, A. Bernard<sup>b</sup>, and V. Garrel<sup>a</sup>

<sup>a</sup>Gemini Observatories, Casilla 603 La Silla, Chile

<sup>b</sup>Aix Marseille Université, CNRS, LAM (Laboratoire d'Astrophysique de Marseille) UMR  
7326, 13388 Marseille, France

## ABSTRACT

We present deep Ks band Gemini GeMS/GSAOI observations of Westerlund 1, the most massive young Galactic star cluster known. The high spatial resolution combined with a relatively stable point spread function across a large field of view provide unique possibilities to resolve the low-mass content of the cluster. We show that the clean point spread function is crucial in handling the source detection in this crowded field suffering extremely high contrast from the brightest hypergiants in the cluster to faint brown dwarfs.

**Keywords:** star clusters: Westerlund 1, Initial Mass Function, Photometry, MCAO, Laser Guide Star Systems

## 1. INTRODUCTION

Much progress has been made in the last decades in our understanding of low-mass star forming regions. Detailed observations of individual objects have made it possible to characterise them in detail and to determine the star formation history and the impact of environment.

Similar studies of massive star clusters (more than  $10^4 M_{\odot}$ ) are much less detailed. However, they differ fundamentally from nearby regions in terms of their central densities and large content of massive stars that may have influenced the star formation process within the cluster.

These clusters are rare and the nearest ones known are an order of magnitude more distant than the nearby low-mass regions. This, together with their higher densities, means that high spatial resolution observations are necessary to resolve the low-mass content of the clusters. Natural seeing observations, even in the best conditions, have only been able to resolve the stellar content down to  $\sim 0.5 M_{\odot}$ <sup>1</sup> in the Galaxy and the Magellanic Clouds.<sup>2,3</sup>

Natural guide star Adaptive Optics (AO) observations have been attempted in the past for several clusters.<sup>4</sup> However, the typical cluster size on the sky is several arcminutes and the isoplanatic angle is substantially smaller in the near-infrared making it unfeasible to observe the whole cluster. Further, these clusters are in the Galactic plane and are thus heavily extinguished making usable natural guide stars relatively rare further complicating a complete mapping. Observations covering the whole cluster are necessary since the cluster content can be mass segregated. Observing just one or a few small regions would provide a highly biased view.

*HST* observations fare better now with the advent of WFC3. The clusters can be covered in one or a few pointings. However, the observations are limited to relatively short wavelengths ( $1.6 \mu\text{m}$  or less) and thus cannot probe any circumstellar disks around the low-mass stars and the effects of extinction still limits the observations. Further, with a mirror size of 2.5 metre, the diffraction limited observations can reach a spatial resolution of  $0.15''$  at the H band.

Future extremely large telescopes can with Adaptive Optics obtain much better spatial resolution. However, already now is it possible to reach good performance over relatively large fields of view from the ground using Multiconjugate Adaptive Optics.<sup>5,6</sup> In particular the advent of laser correcting systems have opened up substantial parameter space previously not reachable.

---

Further author information: (Send correspondence to M. Andersen)  
M. Andersen: E-mail: manderse@gemini.edu

Here we present Gemini GeMS/GSAOI<sup>7,8</sup> imaging of a region in the supermassive young Galactic star cluster Westerlund 1. Westerlund 1 is the most massive young Galactic starcluster known and is thus a prime target to search for variations in the star formation process as a function of environment. In addition it is a very good technical test case for MCAO observations due to the large dynamic range necessary for the observations and the necessity for a stable PSF across the field of view.

We outline the observations, their reduction and calibration. A comparison with H band *HST* observations is performed to show the improvement in source detection for this high contrast crowded region. Finally we discuss the serendipitous discovery of HII regions within the cluster region.

## 2. GEMS/GSAOI OBSERVATIONS

Westerlund 1 was observed on May 22 and May 25 2013. The region chosen was 1 arcminute to the south-west of the cluster center to avoid strong saturation from the brightest supergiants there and to provide suitable natural guide stars. One pointing covering  $85''$  was observed in both the Ks and Br $\gamma$  bands with small offsets to cover the detector gaps and other cosmic blemishes in the arrays. 15 individual integrations of 60 seconds each were obtained for a total on-source integration time of 900 seconds for most of the region. The location of the field observed is shown in Fig. 1

Three natural guide stars were suitable for corrections and were reasonably well spread across and around the field as shown in Fig. 1. Three natural guide stars provide the possibility of an astrometric solution for the field and their wide separation provides the possibility of a stable PSF across the field.

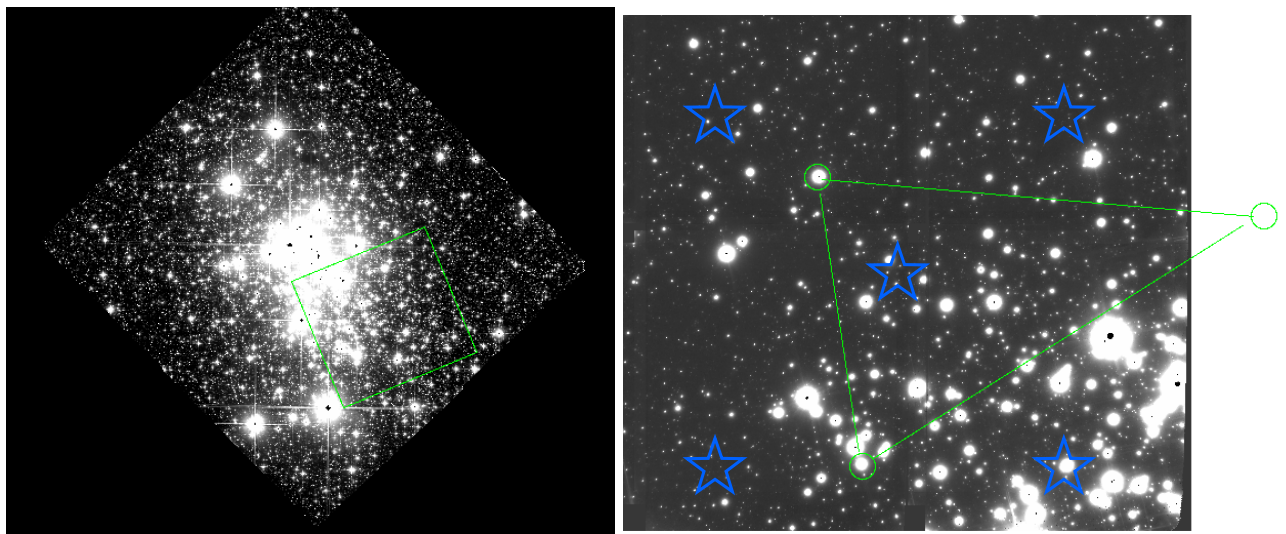


Figure 1. Left: HST WFC3 F160W (similar to an H band) mosaic of Wd1. The field of view is  $5'$  square. The brightest stars in the frame are H $\sim 6$  (all heavily saturated in the HST observations) and the faintest detected H $\sim 22$ . The spatial resolution is  $0''.15$ . Shown as the green box is the field observed with GeMS/GSAOI. Right: The GeMS/GSAOI mosaiced Ks band observations. The field of view is  $85''$  square. Shown are the locations of the laser on the sky (stars) and the location of the three natural guide stars (circles). The faintest stars visible have a Ks band magnitude of  $\sim 20.5$ .

The data were reduced in a standard manner using dedicated sky frames to remove the variable sky background. The sky position was chosen sufficiently close that the laser propagation did not have to be stopped and re-acquired when back on the science field. A basic distortion model was applied to each quadrant in the array before all the frames were co-added.<sup>6</sup> Some time variable distortion is known for GSAOI observations. However, since we here are only focused on the photometry the residual distortion does not interfere with the results presented here.

The spatial resolution in the Ks band image varies slightly across the field but is 80-100 mas for most of the region. For comparison the HST F160W images have a diffraction limit of  $0.15''$ . The improvement is crucial for

crowded field photometry. Both the quality of the photometry and the depth of the data where most of the faint stars can still be identified depend on the level of crowding. The level where half the stars at a given magnitude are detected is much higher in high density clusters than what would be expected from sparse fields.<sup>2,9</sup>

Photometry was performed using the `allstar` package within the `pyraf` environment. `allstar` performs point spread function (PSF) photometry using a PSF created from the frame. Here we allowed for a simple first order variation in the PSF across the full GSAOI/GeMS field of view.

Obtaining the photometry is complicated by the spatially varying PSF across the field-of-view. Although the MCAO system provides a more stable PSF than previous smaller field of view single guide star AO systems there is still some spatial variations. The first order PSF model does account partially for this. However, we still find that there is residuals of  $\sim 5\%$  across the field of view compared to the ground-based data.<sup>10</sup> A higher order fit to the PSF will be necessary to directly correct for this effect.<sup>11</sup>

The photometry was zero point calibrated to the previously obtained ground-based SOFI observations.<sup>10,12</sup> These observations were already placed on the 2MASS system so in effect the observations are calibrated to 2MASS magnitudes. A direct calibration to 2MASS is not feasible due to the very large difference in depth and spatial resolution between the two datasets.

In addition to the Ks band data shown in Fig. 1, data in the J and H bands were obtained as well as Brackett  $\gamma$  narrow band observations. Here we focus on the Ks and Brackett  $\gamma$  data. The main reasons are that the data complements very well the already obtained HST data which only extends to  $1.6 \mu\text{m}$ . The early J and H band observations from GeMS/GSAOI unfortunately suffered from some partially corrected images, resulting in a slightly triangular PSF shape. As we discuss below the shape and relative stability of the PSF are crucial in crowded fields and we opted to use the HST observations for the short wavelength data.

### 3. SOURCE DETECTION AND PHOTOMETRY

Fig. 2 shows a comparison between the same field of view obtained with HST in the F125W band, corresponding to a J band filter, and GeMS/GSAOI in the Ks band. The field of view is  $45'' \times 60''$ .

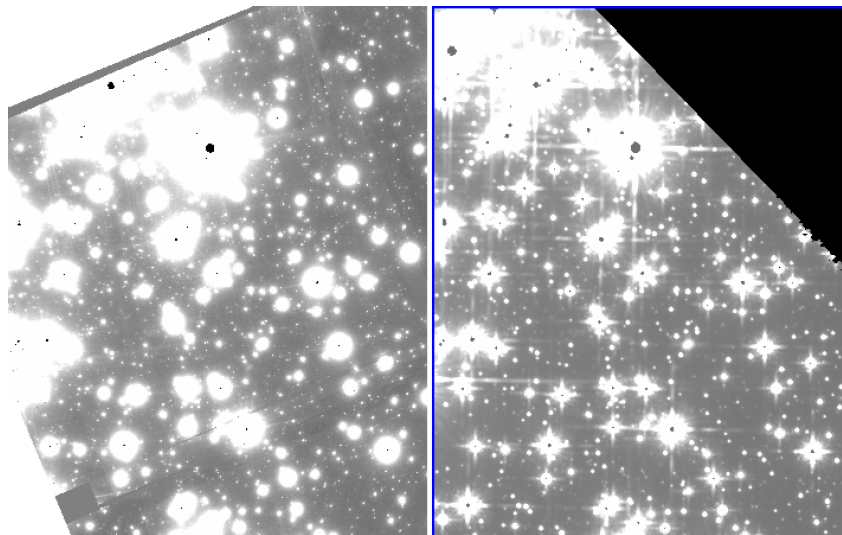


Figure 2. A comparison of the Ks band GSAOI image (left) and the F125W band HST image (right). Even though the spatial resolution is comparable (slightly worse in the F125W band) is the cleaner PSF of the GSAOI observations helping to resolve many more faint stars, especially close to bright stars.

The spatial resolution is somewhat worse in the HST F125W band ( $0''.13$ ) than in the Ks band with GSAOI. However, in addition to a slightly wider PSF there are also substantial structure in the PSF that makes source detection complicated and introduce additional blending effects. The diffraction rings are broken into spots

which can mimic point sources and have to be taken into account, either through multi-color photometry that can exclude them through their spatial position or through manual inspection. In addition light is scattered along the spiders holding the secondary complicating the source identification further. This is less of a complication for the GSAOI data. The PSF is smooth as a function of radius which makes source detection relatively straight forward compared to the HST photometry.

The difference can be seen in Fig. 3 where the sources detected in the HST F125W and F160W images are compared with the sources detected in the GSAOI Ks band image. For the HST, identification was required in both bands in order for the source to be considered real due to the spurious detections. Even with a conservative

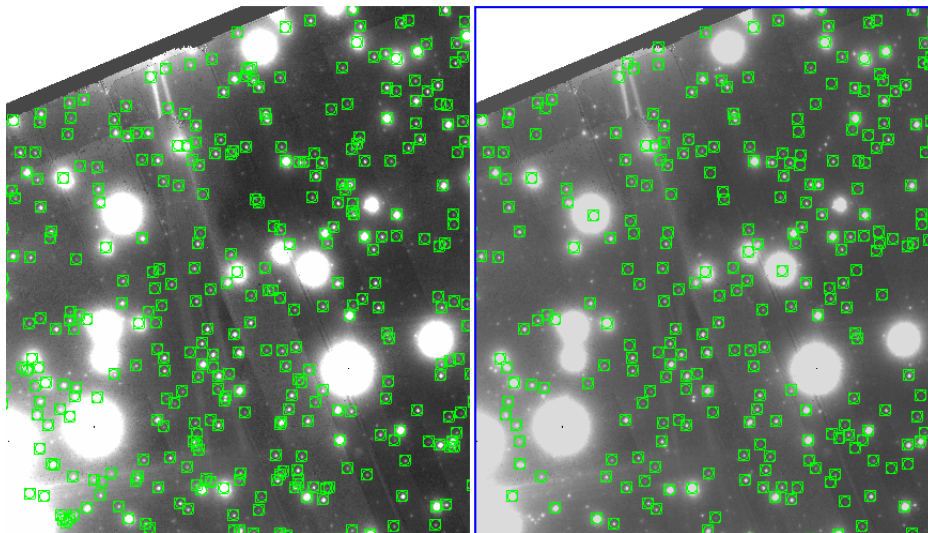


Figure 3. A comparison between a conservative source detection for the GSAOI image (left) with the sources detected in the HST survey (right). The conservative cut of  $10\sigma$  was chosen to avoid false detections since only one band was available. Numerous faint sources are detected in the GSAOI image that were missed in the HST images mainly due to crowding and PSF features.

detection threshold there are substantially more faint sources detected than was the case in the HST survey. This is true both in terms of sensitivity to faint objects and the lack of structure in the PSF for GeMS/GSAOI.

Future H band observations will together with the current Ks band data allow a much deeper study of Westerlund 1 and will allow to probe the cluster mass function both to lower masses overall but equally important probe the low-mass mass function closer to the cluster center. Fig. 4 compares the source counts between the HST and GSAOI images. The increased depth compared to the HST data suggests that the brown dwarf limit can be reached with the GeMS/GSAOI observations compared to  $0.15 M_{\odot}$  for the HST data (where the depth is the magnitude limit where 50% or more of the sources are detected<sup>9</sup>). The extended depth is crucial since the mass function is then traced well beyond the peak mass of the field star IMF and it can conclusively be determined if the IMF in a massive star cluster is similar to that of the field.

#### 4. HII REGIONS ALONG THE LINE OF SIGHT

Our current knowledge of massive star cluster formation is limited. In particular, the time scale over which the cluster is formed is unclear; whether it happens on a time scale comparable with the free fall time of the region over many free fall times.<sup>13</sup>

One crude approach to gauge the age distribution is the near-infrared color-magnitude diagram and estimate how much of the scatter can be attributed to an age spread.<sup>14</sup> did this for Wd1 and suggested the age spread is low compared to the age of the cluster (less than 1 Myr for a 3-5 Myr old cluster). Further, the general Wd1 cluster appears void of large amounts of gas and dust. There is a small gradient of extinction across Wd1 but it



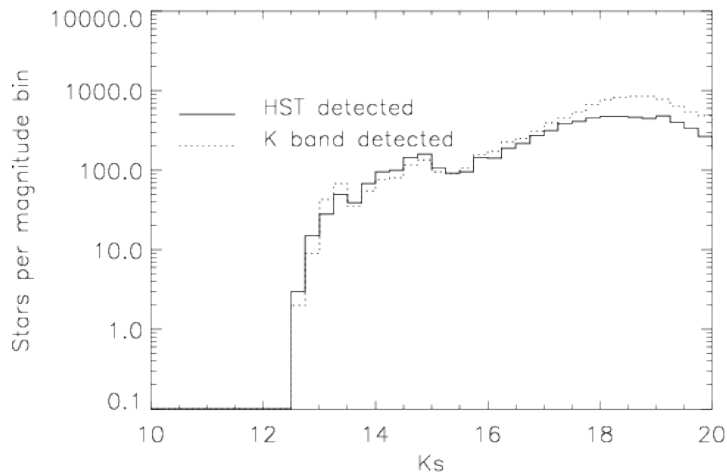


Figure 4. A comparison of the source count from sources detected in the Ks band alone (dotted histogram) versus the sources detected in the F125W and F160W bands (solid histogram).

only corresponds to  $A_V$  of 1 and due to its smooth variation is likely related to slow variations in the foreground extinction and not internal.<sup>9</sup>

However, there appears to be some diffuse emission present in the images. This is particularly strong in the Bracket  $\gamma$  images as shown in Fig. 5. The high spatial resolution clearly shows the structure of the diffuse emission surrounding the bright star in the center of it. There has previously been discovered diffuse emission within Wd1<sup>15</sup> but this was associated with an evolved star. In this case the emission seems to spatially correlate with a  $100\ \mu\text{m}$  *Herschel* source suggesting heating dust from e.g. an HII region. Further, there is weak diffuse emission in the F125W and F160W bands as well as in the *Spitzer* IRAC bands suggesting other emission lines and PAH emission.

Intermediate resolution optical spectroscopy of the diffuse emission has shown strong  $H_\alpha$  and  $[SII]$  lines strongly suggesting it is an HII region. The radial velocity was found to be similar to that of Wd1<sup>16</sup> confirming they are spatially close to each other. This in turns questions how isolated Wd1 is and if there is star formation in its immediate vicinity.

## REFERENCES

- [1] Stolte, A., Brandner, W., Brandl, B., and Zinnecker, H., “The Secrets of the Nearest Starburst Cluster. II. The Present-Day Mass Function in NGC 3603,” *AJ* **132**, 253–270 (July 2006).
- [2] Andersen, M., Zinnecker, H., Moneti, A., McCaughrean, M. J., Brandl, B., Brandner, W., Meylan, G., and Hunter, D., “The Low-Mass Initial Mass Function in the 30 Doradus Starburst Cluster,” *ApJ* **707**, 1347–1360 (Dec. 2009).
- [3] Gouliermis, D., Brandner, W., and Henning, T., “The Initial Mass Function toward the Low-Mass End in the Large Magellanic Cloud with Hubble Space Telescope WFPC2 Observations,” *ApJ* **623**, 846–859 (Apr. 2005).
- [4] Eisenhauer, F., Quirrenbach, A., Zinnecker, H., and Genzel, R., “Stellar Content of the Galactic Starburst Template NGC 3603 from Adaptive Optics Observations,” *ApJ* **498**, 278–292 (May 1998).
- [5] Rigaut, F., Neichel, B., Boccas, M., d’Orgeville, C., Vidal, F., van Dam, M. A., Arriagada, G., Fesquet, V., Galvez, R. L., Gausachs, G., Cavedoni, C., Ebberts, A. W., Karewicz, S., James, E., Lührs, J., Montes, V., Perez, G., Rambold, W. N., Rojas, R., Walker, S., Bec, M., Tranco, G., Sheehan, M., Irarrazaval, B., Boyer, C., Ellerbroek, B. L., Flicker, R., Gratadour, D., Garcia-Rissmann, A., and Daruich, F., “Gemini multiconjugate adaptive optics system review - I. Design, trade-offs and integration,” *MNRAS* **437**, 2361–2375 (Jan. 2014).

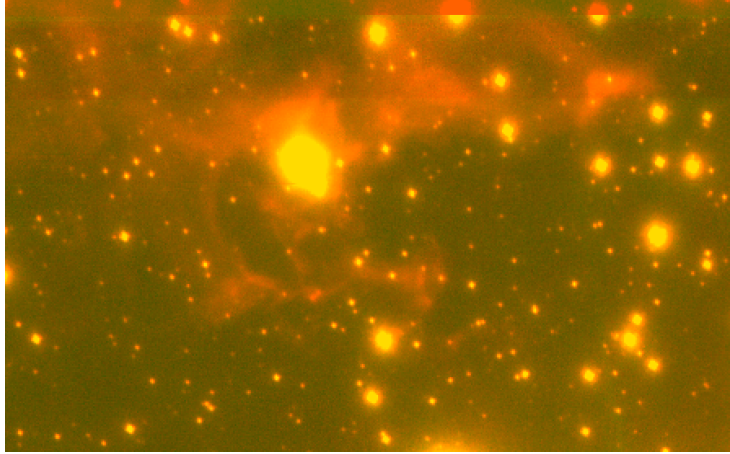


Figure 5. A GeMS/GSAOI Ks and Brackett  $\gamma$  color composite of an HII region discovered with the GSAOI field-of-view. The region is also seen as hot dust in *Herschel* maps and  $H\alpha$  is detected through spectroscopy. The radial velocity is found to be similar to that of the cluster<sup>16</sup> suggesting they are located at the same place in the Galaxy.

- [6] Neichel, B., Lu, J. R., Rigaut, F., Ammons, S. M., Carrasco, E. R., and Lassalle, E., “Astrometric performance of the Gemini multiconjugate adaptive optics system in crowded fields,” *MNRAS* **445**, 500–514 (Nov. 2014).
- [7] Carrasco, E. R., Edwards, M. L., McGregor, P. J., Winge, C., Young, P. J., Doolan, M. C., van Harmelen, J., Rigaut, F. J., Neichel, B., Trancho, G., Artigau, E., Pessev, P., Colazo, F., Tigner, J., Mauro, F., Lührs, J., and Rambold, W. N., “Results from the commissioning of the Gemini South Adaptive Optics Imager (GSAOI) at Gemini South Observatory,” in [*Society of Photo-Optical Instrumentation Engineers (SPIE) Conference Series*], *Society of Photo-Optical Instrumentation Engineers (SPIE) Conference Series* **8447**, 84470N (July 2012).
- [8] McGregor, P., Hart, J., Stevanovic, D., Bloxham, G., Jones, D., Van Harmelen, J., Griesbach, J., Dawson, M., Young, P., and Jarnyk, M. A., “Gemini South Adaptive Optics Imager (GSAOI),” in [*Ground-based Instrumentation for Astronomy*], Moorwood, A. F. M. and Iye, M., eds., *Society of Photo-Optical Instrumentation Engineers (SPIE) Conference Series* **5492**, 1033–1044 (Sept. 2004).
- [9] Andersen, M., Gennaro, M., Brandner, W., de Marchi, G., Meyer, M. R., and Zinnecker, H., “The very low mass stellar content of the young Super-massive Galactic star cluster Westerlund 1,” *A&A*, *accepted*.
- [10] Brandner, W., Clark, J. S., Stolte, A., Waters, R., Negueruela, I., and Goodwin, S. P., “Intermediate to low-mass stellar content of Westerlund 1,” *A&A* **478**, 137–149 (Jan. 2008).
- [11] Turri, P., McConnachie, A. W., Stetson, P. B., Fiorentino, G., Andersen, D. R., Véran, J.-P., and Bono, G., “Toward Precision Photometry for the ELT Era: The Double Subgiant Branch of NGC 1851 Observed with the Gemini/GeMS MCAO System,” *ApJL* **811**, L15 (Oct. 2015).
- [12] Gennaro, M., Brandner, W., Stolte, A., and Henning, T., “Mass segregation and elongation of the starburst cluster Westerlund 1,” *MNRAS* **412**, 2469–2488 (Apr. 2011).
- [13] Tan, J. C., Beltrán, M. T., Caselli, P., Fontani, F., Fuente, A., Krumholz, M. R., McKee, C. F., and Stolte, A., “Massive Star Formation,” *Protostars and Planets VI*, 149–172 (2014).
- [14] Kudryavtseva, N., Brandner, W., Gennaro, M., Rochau, B., Stolte, A., Andersen, M., Da Rio, N., Henning, T., Tognelli, E., Hogg, D., Clark, S., and Waters, R., “Instantaneous Starburst of the Massive Clusters Westerlund 1 and NGC 3603 YC,” *ApJL* **750**, L44 (May 2012).
- [15] Wright, N. J., Wesson, R., Drew, J. E., Barentsen, G., Barlow, M. J., Walsh, J. R., Zijlstra, A., Drake, J. J., Eisloffel, J., and Farnhill, H. J., “The ionized nebula surrounding the red supergiant W26 in Westerlund 1,” *MNRAS* **437**, L1–L5 (Jan. 2014).
- [16] Cottaar, M., Meyer, M. R., Andersen, M., and Espinoza, P., “Is the massive young cluster Westerlund I bound?,” *A&A* **539**, A5 (Mar. 2012).